IAPR Workshop on CV - Special Hardware and Industrial Applications OCT.12-14, 1988, Tokyo

VISUAL INSPECTION IN THE LEATHER INDUSTRY

Patrick Wambacq, Mark Mahy, Geert Noppen, André Oosterlinck

ESAT - MI2
Katholieke Universiteit Leuven
De Croylaan 52 B
3030 Leuven
Belgium

ABSTRACT

The leather industry is one that is certainly in need of automation. As an example we will deal in this paper with the production of leather seats. Many steps in that production process are subject to automation. These include the inspection of the leather hides, stock management, selection of the hides needed for a particular set of seats, nesting of the moulds (taking into account the defects in the leather) and the cutting of the hides. These steps will be explained in somewhat more detail, however the largest part of the paper will be devoted to the automatic visual inspection of the leather. The goal is to detect and describe the hides together with their defects for the subsequent nesting of the moulds. The algorithms presented here are based on the measurement of means, variances and edges, and the application of confidence intervals on them. A few results will be shown.

INTRODUCTION

At the present time the leather industry is not automatized, let alone a few exceptions. The production process is mostly based on hand labour, which results in an output that is heavily depending on subjective criteria. Automation based on visual inspection can lead to an increase in efficiency, a higher productivity and a more stable quality due to objective criteria (computer). The use of computers in the production steps gives the possibility, through the use of statistics, to follow up certain parameters related to the leather. Such a system makes it possible to deliver the designer in an optimal way (gain of materials) the desired hides with the specified characteristics as quality norms and color for every shape or for a part of the shapes (e.g. a lower quality may be tolerated in hidden zones).

The leather hides are delivered in bales of about the same color, coarseness, thickness, texture and quality. At this moment the hides are sorted manually (incoming inspection) and worked up as soon as they are needed. At that time the number of hides satisfying the required shape, quality, color and texture are fetched from the stock and the set of moulds, representing the shapes to be cut out, are taken. The leather hides are spread out on large tables, whereafter the moulds are distributed on the hides. This is done so that the best efficiency is obtained as well as the required quality, taking into account the zones where some small defects and a minor quality are acceptable. Then the leather is cut by hand. All this requires about 6 min for the quality control, 6 min for the optimization of the spreading of the moulds, 6 min for the cutting and 6 min to sort the cut parts. About 75 % of the total area of the leather hide is used.

These steps are certainly good candidates for automation.

The incoming inspection is a first step to automatize, using some kind of vision system. Thereafter, the hides are put in stock, ordered according to their color, texture and quality. Also these manipulations and the stock control are subject to an extensive automation.

The next step to automatize is the detection of the contours of the hide when it is placed on the table to be worked up. These contours constitute the boundary conditions for a subsequent nesting of the moulds.

An automatic visual inspection follows to detect and classify the defective zones or the zones of lower quality. This topic is dealt with in the subsequent sections of this paper.

After the determination of these boundary conditions an automatic nesting of the moulds is started. Therefore, global optimization routines are needed, such as simulated annealing. This will result in savings of material over what a human operator achieves. The last step is then to cut the leather on a X-Y controllable table with a waterjet. Laser cutters are not so adequate here because of focussing problems.

Except for the difficulties of the automatic fault detection and nesting of the moulds, also the needed resolution poses some problems. A leather hide has a typical area of about 4 m^2 and the required level of detail is about one mm. This means that some kind of X-Y controlable table with a matrix or array camera is needed to acquire the images. Due to the size of the hides different subimages will be created during the scanning so that they have to be fit together to form one large image. Also a special vision system with parallel architecture is needed for the storage and fast processing of the images.

The mentioned possibilities of automation are studied by different companies, in a research project founded by the government. The role of our lab is to develop a fast contourfollower and to study methods for the automatic defect detection. In what follows, a defect detection will be treated.

GENERAL CHARACTERISTICS OF THE HIDES

In contrast with automatic fault detection for the most sorts of textiles, no periodic structure is found in hides

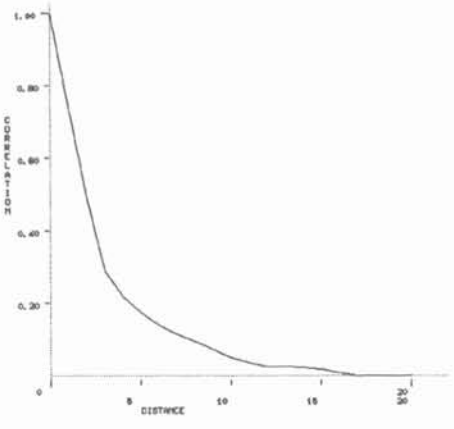

Figure 1: correlation in function of distance (in pixels)

upon which a defect detection can be based. In fact we cannot speak of a real texture, so that defects are mainly found by a statistical analysis of the image data.

Among different hides, a big difference between the mean grey value and the range of the grey values (coarseness) can be present. This depends on the dye with which the hide is colored and on the presence (or absence) of well visible folds of the skin.

Another elementary characteristic of an image is its histogram. However almost none of the faults can be localized using the histogram. Even the presence (or absence) of defects cannot be discovered out of it because as well for faultless parts as for parts with defects the histogram is almost symmetric around a certain grey value.

A histogram is of course not sufficient to characterize the grey value distribution around a given point in the image. This can be represented by the correlation between neighbouring points. As Fig 1 shows, neighbouring points are not uncorrelated, which is probably due to camera defects and correlations present in the hides.

CLASSES OF FAULTS

Faults appear in different forms. They vary from point faults and line defects to bigger faults which run the lenght of a bigger area in the image.

- Point faults

  This fault is often a collection of points with deviations in grey values above or below the mean value of the image, in a localized area of the hide. The dimensions of the points range from 2 to about 5 mm (fig. 2).

- Line defects

  Lines with different thicknesses and lengths are possible. Often a very clear fault center appears, but also lines with the same grey value, barely different from the mean grey value of the neighbourhood occur. The length ranges from 10 mm up to a few cm, the thickness on the other hand from 2 mm to 6 mm (fig. 3 and 4).

- Area faults

  Area faults are visible due to a local deviation in grey value or variance. Different forms and sizes occur (fig. 5).

FAULT DETECTION METHOD

As mentioned in the previous section, the fault detection is mainly based on a statistical analysis of the image of the hide. Also the histogram of an image only appeared to be unsufficient to reach our goal. We could take into account correlations but it is a very time consuming process that would result in a higher price for the system. So the solution has to be relatively fast, but on the other hand it has also to be an adaptive method for the different possible degrees of coarseness and mean values of the images.

Such a possible statistical method can work as follows.

We suppose that the grey values of an image have a gaussian distribution. Such a distribution is given by

$$\mathcal{F}(x) = \frac{1}{\sqrt{2\pi}\sigma} e^{\frac{-(x-\mu)^2}{2\sigma^2}}$$

with

- μ : mean of the image
- σ : standard deviation of the image

This function is characterised by the mean μ and standard deviation σ. So if we calculate the mean and the variance of the good part of the image, the theoretical grey value distribution is known. The next step is to calculate a few characteristics, as mean and variance in a neighbourhood (N X N mask) around a central pixel.

$$mean = \sum_{i=1}^{n} x_i/N$$

$$var = \sum_{i=1}^{n} (x_i - mean)^2/(N-1)$$

Knowing the distribution of the pixels, we can predict the distribution of the calculated characteristics if the pixels in the mask are statistical independent, i.e. gaussian for the mean and chi square for the variance [1]. This last assumption is in fact not true, because neighbouring pixels are correlated. Nevertheless we neglect this at this moment and shall adapt later on the results to this effect. If we know the distribution of the mean and variance, we can handle both characteristics in the same way using confidence intervals.

If we analyse a whole image carefully, we discover faultless parts in the image which have about the same statistical environment with respect to the mean and variance as certain parts of the fault. Due to this it is not possible to detect the whole fault at once, so we are obliged to detect in a first step the centers of the faults, i.e. the most deviating part, of the fault. In a next step we let grow these centers using the features mean and variance (deviations against confidence intervals).

The detection of the center parts of faults determines if parts of the image will be classified incorrectly or not. So this classification has to be done very acurately. We have detected those center parts using three contributions.

- Mean contribution

  This part is obtained using a more severe confidence interval than for the determination of the total fault. Possible noise is eliminated using a M X M mask centered around a wrong classified pixel. Only if the number of wrong detected pixels in this mask is above a certain threshold, the central pixel belongs to the central faults.

- var contribution

  This part is obtained in the same way as the mean contribution.

- edge contribution

  The edges in an image are calculated as the angle between the edge space and the 9-dim vector representing a 3X3 mask of the image. This is done by choosing a 9 dim orthonormal basis for the 3X3 mask vectorspace [2]. The edge is given by

$$edge = \frac{variance - 9 \times mean^2}{variance}$$

  As can be easily verified, this edge measure is independent for rescaling factors, which is not the case for shifts compare the edges of different images, the mean grey value of those images has to be the same. We shift therefore every image to a certain mean.

  When we have calculated the edges of the image, the edges are thresholded. This threshold is chosen in such a way that in faultless images no points remain after the elimination of noise (eliminated in the same manner as in the previous two cases) in the thresholded image. If there is no edge detection, there is no contribution to the central faults, otherwhise, the mean and variance of the edge image is calculated and the edges are normalised as follows

$$edge = 15 \times \frac{edge - mean}{\sqrt{variance}}$$

  Finally those values are thresholded, and noise is eliminated (again in the same way as in the previous two cases). The remaining pixels belong to central faults due to the edge measure. This can only be done if the image of which the edges are calculated is properly shifted.

PRACTICAL IMPLEMENTATION

Two important adaptations still have to be done

- Preprocessing of the images

  Our images are recorded using a matrix camera. With such a system often a light reflection occurs in the images. To eliminate this reflection the images are approximated row by row and column by column with a parabolic function. The rescaled difference between the approximation and the row or column yield an image without disturbing reflextions. If the fault lies along a row or a column this method gives poor results, but in the final system the images will be recorded using an array camera so that this effect is at least reduced. In a next step, noise is eliminated using a median filter and the image is subsampled to eliminate eventually camera defects (partial decorrelation of the image).

- Adaption of the model to correlated values

  Instead of calculating each time the confidence interval, the images are normalized in such a way that the grey values have a gaussian distribution with mean 0 and variance 1. This is also necessary to adapt the value corresponding to the given confidence interval due to the correlation between neighbouring pixels. Because the correlation is now approximatively the same for the different normalized images, the problem is reduced to find empirically a threshold for those images.

RESULTS

All the different thresholds and mask sizes are found empirically. It was possible to choose them in such a way that in very few cases overdetection occurs and that only two classes of faults aren't found. These are line faults without an important central part and point faults with small dimensions ($\pm$ 1 à 2 mm) (fig. 2 and 4). These faults are however very weak and are difficult to find because they have the same statistical environment as in some faultless parts of the image. The weak line faults are relatively good visible because human eyes are very sensitive to lines. They are not found by this method due to the repetition along a line of about the same statistical environment of 5 by 5 pixels (the chosen mask size), which contains no deviations against the measured characteristics. In figures 2 to 5 some preprocessed images are shown together with the corresponding fault detection. To improve the visibility of the faults, all the images are rescaled to the maximum range. The mean and variance of the total recorded images (mean_t and var_t) and of the good parts in those images (mean_g and var_g) is each time specified.

ACKNOWLEDGMENT

The authors wish to thank I.W.O.N.L. for the founding of the research and the cooperating companies for their support to the project.

REFERENCES

[1] Graf/Henning/Stange, 'Formeln und Tabellen der mathematischen Statistik',Springer-Verslag, berlin/heidelberg/New York

[2] W. Frey and Chung-Ching Chen, 'Fast boundary detection:A generalisation and a new algorithm', IEEE trans. on comp. oct. 1977, pp. 556-566

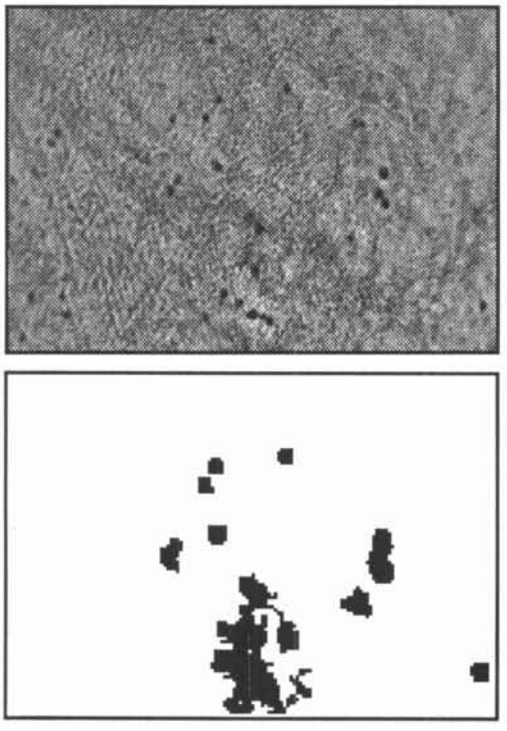

Figure 2: example of point faults with the corresponding fault detection, mean_t = 74.5, var_t = 28.9, mean_g = 74.8, var_g = 19.9

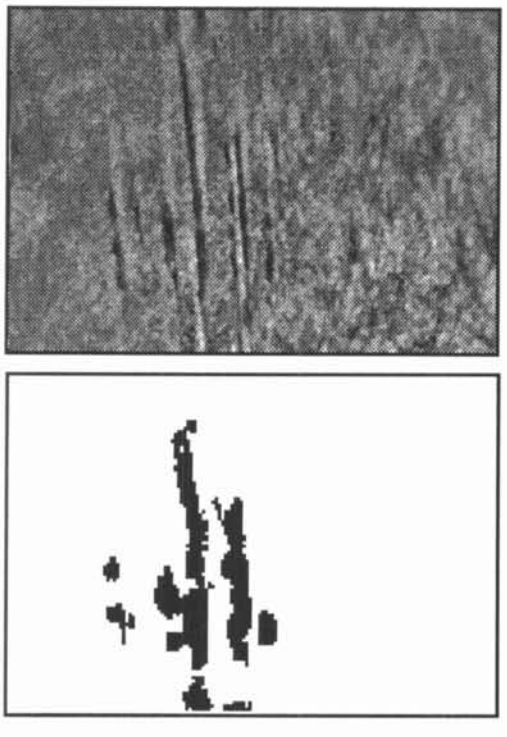

Figure 3: example of line faults with the corresponding fault detection, mean_t = 92.1, var_t = 13.7, mean_g = 92.2, var_g = 10.3

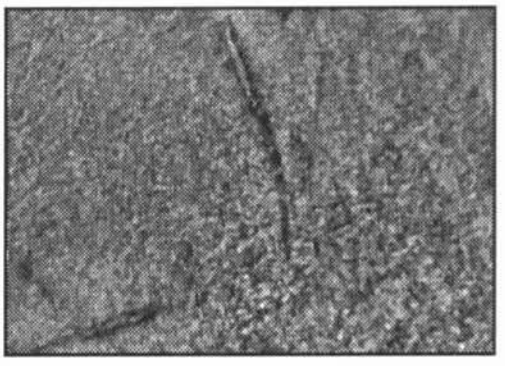

Figure 4: example of barely visible line faults, no faults are detected mean_t = 68.8, var_t = 13.6, mean_g = 69.0, var_g = 11.5

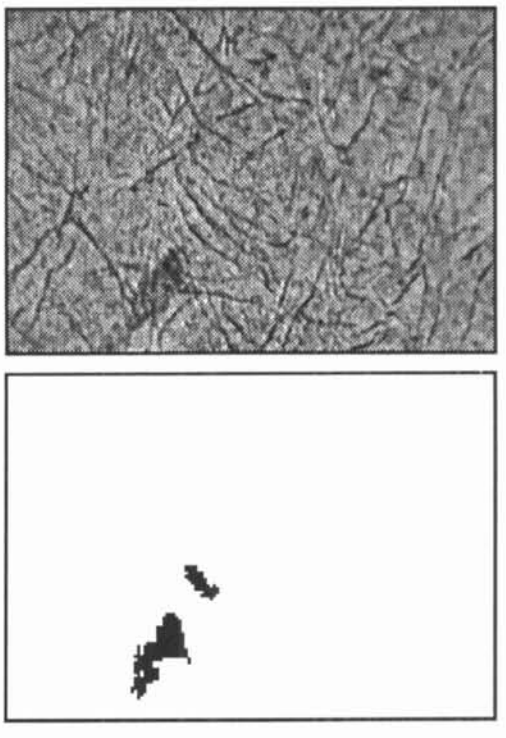

Figure 5: example of an area fault (mean deviation) with the corresponding fault detection, mean_t = 87.5, var_t = 28.9, mean_g = 87.7, var_g = 28.4